LPV Modeling and Control for Active Flutter Suppression of a Smart Airfoil

Ali M. H. Al-Hajjar* and Ali Khudhair Al-Jiboory†
Michigan State University, East Lansing, MI 48823, USA
Sean Shan-Min Swei‡
NASA Ames Research Center, Moffett Field, CA 94035, USA
Guoming Zhu§
Michigan State University, East Lansing, MI 48823, USA

In this paper, a novel technique of linear parameter varying (LPV) modeling and control of a smart airfoil for active flutter suppression is proposed, where the smart airfoil has a groove along its chord and contains a moving mass that is used to control the airfoil pitching and plunging motions. The new LPV modeling technique is proposed that uses mass position as a scheduling parameter to describe the physical constraint of the moving mass, in addition the hard constraint at the boundaries is realized by proper selection of the parameter varying function. Therefore, the position of the moving mass and the free stream airspeed are considered the scheduling parameters in the study. A state-feedback based LPV gain-scheduling controller with guaranteed $\mathscr{H}_\infty$ performance is presented by utilizing the dynamics of the moving mass as scheduling parameter at a given airspeed. The numerical simulations demonstrate the effectiveness of the proposed LPV control architecture by significantly improving the performance while reducing the control effort.

Nomenclature

b	Typical section semi-chord (the length of the groove).
c	Typical section chord.
C_L	Lift coefficient.
C_{L_α}	$(\frac{dC_L}{d_\alpha})$, C_{L_α} =2π.
e	Elastic axis (e.a) from elastic aerodynamic center, aft positive.
$\bar{e}$	Nondimensional e (e/b).
$F_a(t)$	Aerodynamic loads induced by airfoil motion.
g	Gravity constant.
$\bar{g}$	Nondimensional g $(\frac{g}{\omega_\alpha^2 b})$.
h	Plunging displacement.
$\bar{h}$	Nondimensional plunging displacement $(\frac{h}{b})$.
I_α	Mass moment of inertia about e.a. per unit span.
K_h	Spring constant for plunging mode.
K_α	Spring constant for pitching mode.
M	Mass per unit spa of the typical section.
m	Mass of the control device.
q_p	Dynamic pressure $(\frac{\rho V^2}{2})$.
r_α	Radius of gyration about e.a. $(\sqrt{\frac{I_\alpha}{Mb^2}})$.
t	Time.

*PhD. Student, Mechanical Engineering, AIAA Student Member. alhajjar@msu.edu
†Post-doc, Mechanical Engineering. aljiboor@msu.edu
‡Senior Research Scientist, Intelligent Systems Division, Associate Fellow. sean.s.swei@nasa.gov.
§Professor, Mechanical Engineering, Electrical and Computer Engineering. zhug@egr.msu.edu

u Control input.
$\bar{u}$ Nondimensional control input $(\frac{u}{M\omega_\alpha^2 b})$.
V Free stream airspeed.
$\bar{V}$ Nondimensional free stream airspeed $(\frac{V}{\omega_\alpha b})$.
x_α Static unbalance, distance from e.a. to inertia axis, aft positive.
$\bar{x}_\alpha$ Nondimensional static unbalance $(\frac{x_\alpha}{b})$.
y Displacement, traveling distance of control mass m.
$\bar{y}$ Nondimensional displacement $(\frac{y}{b})$.
α Angel of incidence, positive nose up.
α_S α for small I.C.
α_L α for large I.C.
β Mass ratio, Control device to the airfoil $(\frac{m}{M})$.
θ_1 First scheduling parameter.
θ_2 Second scheduling parameter, free stream airspeed $(\bar{V})$.
θ_3 Third scheduling parameter, free stream airspeed squared $(\bar{V}^2)$.
μ Mass ratio of the typical section to the apparent mass $(\frac{M}{\pi\rho b^2})$.
ω_h Uncoupled plunging natural frequency.
ω_α Uncoupled pitching natural frequency.
ρ Air density.
τ Nondimensional time $(\omega_\alpha t)$.

I. Introduction

ACTIVE flutter suppression has been a critical research topic in aerospace applications for many decades, especially, as the emerging air vehicle structures become highly flexible, active flutter suppression becomes a key technical design requirement. Decreasing the aircraft weight, improving the aerodynamic efficiency, and increasing the critical flight speed continue to be the main thrusts for future aeronautical research. There are many methods and designs in literature concerning suppression of flutter phenomena. Passive methods have been used to solve this problem for many years, however, these methods lead to increased aircraft mass that is undesirable; see references.[?,?,?,?] It is clear that passive methods are not prolific. On the other hand, active control techniques can provide crucial and liable solutions that not only increase the aircraft critical speed and suppress the oscillations but also decrease the aircraft weight with enhanced efficiency and performance.

There are many active control techniques in literature for suppressing and reducing flutter. Using piezoelectric actuation to control flutter was given by Han et al.,[?] where numerical and experimental investigation were conducted for active flutter suppression of a sweptback cantilevered lifting surface. Finite element analysis, panel aerodynamics, and the minimum statespace realization were used to develop the equation of motion that is used for system analysis and control design. H_2 and μ-synthesized control laws were designed and the flutter suppression performance was evaluated in wind tunnel testing. Electro-hydraulic mechanical actuation of control surfaces,[?] reaction jets,[?] jet flaps, micro-flaps[?] were also introduced as active flutter suppression techniques. C. De Marqui et al.[?] developed a flexible mounting system for flutter tests with rigid wings in a wind tunnel. This flexible mount system represents a two-degree-of-freedom system with rigid wings encountering flutter. An aeroelastic model was formulated to simulate the aeroelastic behavior of the corresponding system and a state feedback control was designed for this model. The wind tunnel test model was a rectangular wing with an NACA 0012 airfoil section and with a trailing edge control surface actuator. The main goal was to suppress flutter and to maintain the stability of the closed-loop system. Zhang and Behal[?] introduced a continuous-time controller to suppress the aeroelastic vibrations of the wing section model in an unsteady aerodynamic incompressible flow. The flap hinge torque of a trailing-edge flap surface was used as the control input. Their control design was based on the choice of the pitching angle as the output variable. The closed-loop system was shown to be robust to external disturbances. Also, numerical simulation results showed the efficacy of the method in suppressing aeroelastic vibrations in both pre- and post-flutter flight regimes under multiple external disturbances.

A special attention was given to linear parameter-varying (LPV) modeling and control of airfoils. For example,

Wingerden et al.[?] exploited a system identification algorithm for an LPV aeroelastic system equipped with trailing edge flaps, where a factorization was used to form predictors based on past inputs, outputs, and known aeroelastic data, and these predictors were used to estimate the state sequence and to form LPV aeroelastic system matrices. Since the algorithm can be used in a closed-loop setting it can be applied to flutter suppression problems. Barker and Balas[?] designed two-parameter (LPV) gain-scheduled controllers for active flutter suppression of the Benchmark Active Control Technology (BACT) wing section at NASA Langley Research Center. The results were compared to a previously designed gain-scheduled controller. The BACT wing section dynamics changes significantly as a function of Mach number and dynamic pressure. The two-parameter LPV gain-scheduled controllers incorporate these changes as well as bounds on the rate of change of Mach number and dynamic pressure. The inclusion of rate bounds in the design process allows for improved performance over a larger range of operational conditions than previously designed gain-scheduled controller based on linear fractional transformation. These LPV controllers reduce coupling among the trailing-edge flap, the pitch and plunge modes, and optimize wind gust attenuation. Closed-loop stability and improved performance were demonstrated via time-domain simulations with varying Mach number and dynamic pressure. Lau and Kerner[?] utilized a standard linear model for the control of a thin airfoil under subsonic flow. The two-dimensional section airfoil was modeled with three degrees of freedoms: plunge, pitch and flap angle, resulting a six dimensional linear system. The system has three inputs: the torque applied at the flap hinge, the lift and moment generated by the air flowing over the wing. The one dimensional control is the additional torque that can be applied at the hinge through a motor. The goal was to use feedback to stabilize the airfoil at or above its flutter speed with several control strategies. Chen et al.[?] developed LPV aeroservoelastic model with nonlinear aerodynamics based on adaptive method. The LPV controller was then designed to suppress flutter with good accuracy and robustness. It turns out that the LPV controller also provides a good tool for virtual flutter flight experiments. Balas et al.[?] designed aeroservoelastic controllers using H_∞ and LPV control design techniques for a Body Freedom Flutter (BFF) aircraft and compared the performances of the controllers in both frequency and time domain simulations. Though the performance was acceptable, the designed LPV controller was not able to achieve the same level of performance as from individual $\mathscr{H}_\infty$ controller. From the literature review, one can see that the conventional LPV model considers the scheduling parameter as a physical parameter of the system matrices that changes with time,[?,?,?] whereas the quasi-LPV model[?,?,?] considers systems with one or more states in the system matrices.

The smart airfoil model proposed by Swei and Jiang[?] is studied in this paper; see Fig.1. The smart airfoil is a two dimensional airfoil with a groove along its chord that contains a moving light mass. The mass is allowed to move along the groove to control and suppress the pitching and plunging motion of the airfoil. The airspeed and position of the moving mass are considered as scheduling parameters in the LPV model and the mass position is used in control design as the scheduling parameter. In this paper, we propose to utilize the scheduling parameter as part of a scaling factor for the smart airfoil model. In particular, the position of moving mass is scaled and parametrized such that it is confined within the length of groove. According to the authors knowledge, this integration of scheduling parameter with scaling of control effector is novel that has never reported in the LPV control literature in the past. The main contribution of this paper is to develop a novel LPV modeling and control technique of the smart airfoil for flutter suppression, with guaranteed $\mathscr{H}_\infty$ performance.

This paper is organized as follows. Section II presents the nonlinear model of the smart airfoil, and the baseline LPV model (LPV-0) and LPV model with parameter scaling (LPV-1). Section III contains problem formulation and controller design. Comparisons and simulation results are presented in Section IV. Conclusions and future work are given in Section V.

II. LPV Modeling of a Smart Airfoil

II.A. Nonlinear model

In this section, the mathematical model of the smart airfoil is presented. The linearized equations of motion of the airfoil aeroservoelastic model can be written as[?]

$$\begin{bmatrix} m+M & Mx_\alpha \\ Mx_\alpha & I_\alpha \end{bmatrix} \begin{bmatrix} \ddot{h}(t) \\ \ddot{\alpha}(t) \end{bmatrix} + \begin{bmatrix} K_h & 0 \\ 0 & K_\alpha \end{bmatrix} \begin{bmatrix} h(t) \\ \alpha(t) \end{bmatrix} = \begin{bmatrix} 0 \\ mg \end{bmatrix} y(t) + F_a(t) \tag{1}$$

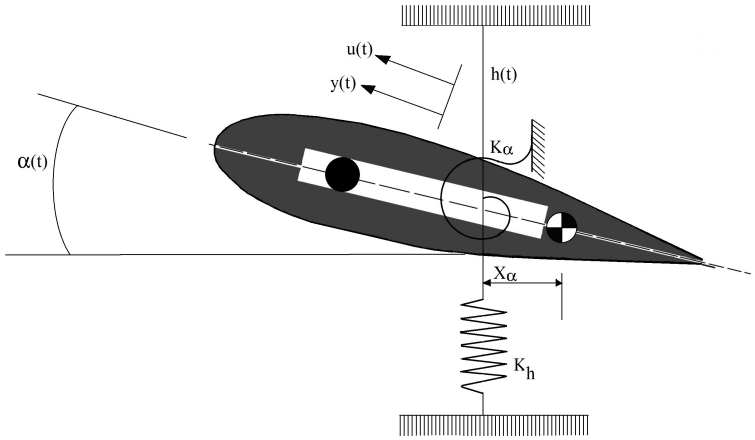

Figure 1: Typical smart airfoil section

$$m\ddot{y}(t) = mg\alpha(t) + u(t) \tag{2}$$

where $F_a(t)$ denotes the aerodynamic loading, m and M the moving mass and airfoil mass, respectively, additional variables and parameters used in (1) and (2) can be found in Fig. 1.[?] It is important to note that the position of moving mass $y(t)$ in (1) can be considered as the control input to the airfoil, whereas $u(t)$ in (2) can be considered as the control input to the moving mass m. The airfoil with such a control device is called "Smart Airfoil".[?] The following quasi-steady aerodynamic load model[?] for $F_a(t)$ is adapted in this study,

$$F_a(t) = P\left(\begin{bmatrix} \frac{-1}{V} & 0 \\ \frac{e}{V} & 0 \end{bmatrix}\begin{bmatrix} \dot{h}(t) \\ \dot{\alpha}(t) \end{bmatrix} + \begin{bmatrix} 0 & -1 \\ 0 & e \end{bmatrix}\begin{bmatrix} h(t) \\ \alpha(t) \end{bmatrix}\right), \quad P = q_p c C_{L_\alpha} \tag{3}$$

Now, substituting (3) into (1) and performing nondimensionalization for all the physical parameters, we obtain the nondimensionalized equations of motion for the smart airfoil model as follows,

$$\begin{bmatrix} 1+\beta & \bar{x}_\alpha \\ \bar{x}_\alpha & \bar{r}_\alpha^2 \end{bmatrix}\begin{bmatrix} \ddot{\bar{h}}(\tau) \\ \ddot{\alpha}(\tau) \end{bmatrix} + \begin{bmatrix} \frac{2\bar{V}}{\mu} & 0 \\ \frac{-2\bar{V}\bar{e}}{\mu} & 0 \end{bmatrix}\begin{bmatrix} \dot{\bar{h}}(\tau) \\ \dot{\alpha}(\tau) \end{bmatrix} + \begin{bmatrix} \frac{\omega_h^2}{\omega_\alpha^2} & \frac{2\bar{V}^2}{\mu} \\ 0 & \frac{-2\bar{V}^2\bar{e}}{\mu} + \bar{r}_\alpha^2 \end{bmatrix}\begin{bmatrix} \bar{h}(\tau) \\ \alpha(\tau) \end{bmatrix} = \begin{bmatrix} 0 \\ \beta\bar{g} \end{bmatrix}\bar{y}(\tau) \tag{4}$$

$$\ddot{\bar{y}}(\tau) = \bar{g}\alpha(\tau) + \bar{u}(\tau) := \tilde{u}(\tau) \tag{5}$$

where $\tau = \omega_\alpha t$ is the nondimensional time. Note that to simplify the notation, the overhead "dot" in (4) and (5) represents the time derivative with respect to τ. When the flutter occurs, the plunging displacement h and pitching angle α are fed back in order to properly position the moving mass m, which generates a damping effect to the airfoil, resulting in reduced flutter and increased the critical flutter speed.

II.B. Proposed LPV plant model: LPV-0

Rearranging (4) and (5) yields the following

$$\begin{bmatrix} \ddot{\bar{h}}(\tau) \\ \ddot{\alpha}(\tau) \end{bmatrix} + \begin{bmatrix} \frac{-2\bar{r}^2\bar{V}}{q\mu} - \frac{2\bar{V}\bar{e}\bar{x}_\alpha}{q\mu} & 0 \\ \frac{2\bar{x}\bar{V}}{q\mu} + \frac{2\bar{V}\bar{e}(1+\beta)}{q\mu} & 0 \end{bmatrix}\begin{bmatrix} \dot{\bar{h}}(\tau) \\ \dot{\alpha}(\tau) \end{bmatrix} + \begin{bmatrix} \frac{-\bar{r}_\alpha^2\omega_h^2}{q\omega_\alpha^2} & \frac{-2\bar{r}_\alpha\bar{V}^2}{q\mu} - \frac{2\bar{V}^2\bar{e}\bar{x}_\alpha}{q\mu} + \frac{\bar{r}^2\bar{x}_\alpha}{q} \\ \frac{\bar{x}_\alpha\omega_h^2}{q\omega_\alpha^2} & \frac{2\bar{x}_\alpha\bar{V}^2}{q\mu} + \frac{2\bar{V}^2\bar{e}(1+\beta)}{q\mu} + \frac{\bar{r}^2(1+\beta)}{q} \end{bmatrix}\begin{bmatrix} \bar{h}(\tau) \\ \alpha(\tau) \end{bmatrix} = \begin{bmatrix} \frac{-\bar{x}_\alpha\beta g}{q} \\ \frac{(1+\beta)\beta\bar{g}}{q} \end{bmatrix}\bar{y}(\tau) \tag{6}$$

$$\ddot{\bar{y}}(\tau) = \bar{g}\alpha(\tau) + \bar{u}(\tau) \tag{7}$$

where $q = -(\bar{r}_\alpha^2(1+\beta) - \bar{x}_\alpha^2)$. Now, we define the augmented state x as

$$x = \begin{bmatrix} \bar{x} \\ x_u \end{bmatrix}, \tag{8}$$

where

$$\bar{x} = \begin{bmatrix} \bar{h} \\ \alpha \\ \dot{\bar{h}} \\ \dot{\alpha} \end{bmatrix} \text{ and } x_u = \begin{bmatrix} \bar{y} \\ \dot{\bar{y}} \end{bmatrix}. \tag{9}$$

Then, (6) and (7) can be described in the state-space representation as follows,

$$\begin{aligned} \dot{x}(t) &= A(\theta(t))x(t) + B_u(\theta(t))\bar{u}(t) \\ y(t) &= C(\theta(t))x(t) + D_u(\theta(t))\bar{u}(t) \end{aligned} \tag{10}$$

where $x(t)$ is the augmented state, $y(t)$ the controlled output, and the system matrices $(A(\theta), B_u(\theta), C(\theta), D_u(\theta))$ are given by

$$A(\theta) = \begin{bmatrix} 0 & 0 & 1 & 0 & 0 & 0 \\ 0 & 0 & 0 & 1 & 0 & 0 \\ \frac{\bar{r}_\alpha^2 \omega_h^2}{q\omega_\alpha^2} & \frac{2\bar{r}_\alpha^2\theta_3}{q\mu} + \frac{2\theta_3\bar{e}\bar{x}_\alpha}{q\mu} - \frac{\bar{r}_\alpha^2\bar{x}_\alpha}{q} & \frac{2\bar{r}_\alpha^2\theta_2}{q\mu} + \frac{2\theta_2\bar{e}\bar{x}_\alpha}{q\mu} & 0 & \frac{-\bar{x}_\alpha\beta}{q} & 0 \\ \frac{-\bar{x}_\alpha\omega_h^2}{q\omega_\alpha^2} & \frac{-2\bar{x}_\alpha\theta_3}{q\mu} - \frac{2\theta_3\bar{e}(1+\beta)}{q\mu} - \frac{\bar{r}_\alpha^2(1+\beta)}{q} & \frac{-2\bar{x}\theta_2}{q\mu} - \frac{2\theta_2\bar{e}(1+\beta)}{q\mu} & 0 & \frac{\beta(1+\beta)}{q} & 0 \\ 0 & 0 & 0 & 0 & 0 & 1 \\ 0 & \bar{g} & 0 & 0 & 0 & 0 \end{bmatrix}, \quad B_u(\theta) = \begin{bmatrix} 0 \\ 0 \\ 0 \\ 0 \\ 0 \\ b_6 \end{bmatrix} \tag{11}$$

$$C(\theta) = \begin{bmatrix} 0 & 0 & 0 & 0 & 1 & 0 \end{bmatrix}, \qquad D_u(\theta) = 0,$$

where θ_2 and θ_3 are the scheduling parameters representing, respectively, the normalized airspeed $\bar{V}$ and its square $\bar{V}^2$. In this study, we consider $\theta_2 \in [0.5, 2.92]$, hence $\theta_3 \in [0.25, 8.526]$. Furthermore, b_6 is the parameter utilized to properly constraining the position of the moving mass at the boundaries. To formulate an LPV-0 plant model without a position constraint, we set the parameter $b_6 = 1$. This LPV-0 model will be used to assess the closed-loop system performance.

II.C. Proposed LPV control design model: LPV-1

Now, we present the LPV control design model, namely, the LPV-1 model, which will be used to develop the LPV controllers. The proposed LPV-1 model is based on the LPV-0 model described in (10) and (11), but with $\theta_1 = b_6$ as an additional scheduling parameter to constrain the moving mass. In particular, θ_1 is a function of $\bar{y}$, i.e. $\theta_1 = f(\bar{y})$, and it is devised such that

$$\begin{cases} \theta_1 = 1, & \text{if } \bar{y} \in [-0.35, 0.35] \\ \theta_1 \bar{y} = 0.35, & \text{if } \bar{y} > 0.35 \\ \theta_1 \bar{y} = -0.35, & \text{if } \bar{y} < -0.35 \end{cases}$$

It is clear from the first condition given above that when $\bar{y} \in [-0.35, 0.35]$ and $\theta_1 = 1$, the LPV-1 model will be equivalent to the LPV-0 model. The purpose of the second and third condition is to impose a constraint on the moving mass when it travels beyond ± 0.35, by modulating the control gains through θ_1. The variation of θ_1 as function of the position of the moving mass is illustrated in Fig. 2. This approach may introduce a slight conservativeness to the control design, it is intuitively appealing and proved to be effective.

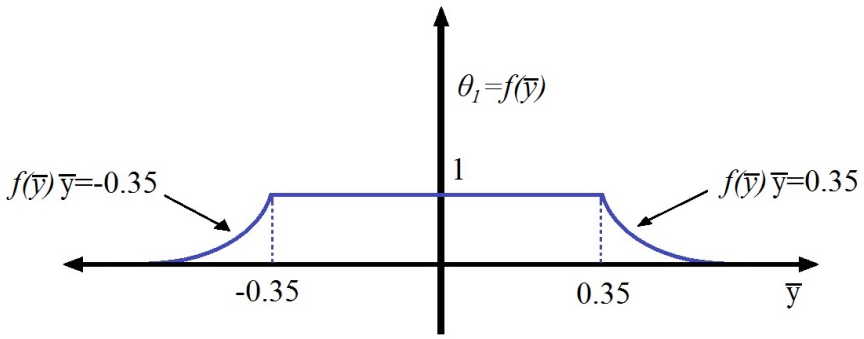

Figure 2: Saturation function

III. LPV Controller Formulation

In this section, we develop a state-feedback based gain scheduling LPV controller for LPV-0 and LPV-1 models with added disturbance input. We consider the following LPV state-space systems,

$$\begin{aligned} \dot{x}(t) &= A(\theta(t))x(t) + B_u(\theta(t))\bar{u}(t) + B_w(\theta(t))w(t) \\ y(t) &= C(\theta(t))x(t) + D_u(\theta(t))\bar{u}(t) + D_w(\theta(t))w(t) \end{aligned} \tag{12}$$

where $(A(\theta), B_u(\theta), C(\theta), D_u(\theta))$ are as defined in (11), $w(t)$ denotes the disturbance input, $B_w = [0\ 0\ 0\ 0\ 0\ 0.1]^T$, and $D_w = 0$. The parameters used in this study are shown in Table 1.

Table 1: Parameters used in the paper

Parameter	Value	Parameter	Value
μ	152	β	0.01
$\bar{e}$	0.35	$h(0)$	0
$\bar{x}_\alpha$	0.25	$\alpha_S(0)$, rad	0.01
$\bar{r}_\alpha^2$	0.388	$\alpha_L(0)$, rad	0.6
b, in	5	$\dot{h}(0)$	0
ω_α, rad/sec	64.1	$\dot{\alpha}(0)$	0
ω_h, rad/sec	55.9	flutter airspeed $\bar{V}$	2.92

Note that α_S and α_L denote small and large initial pitch angles, respectively.

III.A. Problem Formulation

The LPV model described in (12) is assumed to have affine parameters. For instance, the matrix $A(\theta)$ can be represented by

$$A(\theta(t)) = A_0 + \sum_{i=1}^{q} \theta_i(t) A_i \tag{13}$$

where A_0 and A_i are constant matrices, and q denotes the number of scheduling parameters. The scheduling parameter vector $\theta(t)$ is defined as

$$\theta(t) = [\theta_1(t), \theta_2(t), \theta_3(t), ..., \theta_q(t)]^T \tag{14}$$

and each θ_i is bounded by

$$\eta_{1,i} \leq \theta_i \leq \eta_{2,i}\,, \tag{15}$$

where $\eta_{1,i}$ and $\eta_{2,i}$ denote the upper and lower bound. Furthermore, these scheduling parameters also have the rate bound given by

$$\mu_{1,i} \leq \dot{\theta}_i \leq \mu_{2,i}\,. \tag{16}$$

The proposed LPV control is to design a state-feedback controller of the form

$$\bar{u}(t) = K(\theta(t))x(t)\,, \tag{17}$$

where $K(\theta)$ asymptotically stabilizes the closed-loop system subject to the $\mathscr{H}_\infty$ norm constraint from the disturbance input w to the performance output y over the entire parameter variation range.
Substituting the controller (17) into (12) yields the closed-loop system representation described by

$$\begin{aligned} \dot{x}(t) &= A_c(\theta(t))x(t) + B_w(\theta(t))w(t) \\ y(t) &= C_c(\theta(t))x(t) + D_w(\theta(t))w(t) \end{aligned} \tag{18}$$

where

$$\begin{aligned} A_c(\theta(t)) &= A(\theta(t))x(t) + B_u(\theta(t))K(\theta(t)) \\ C_c(\theta(t)) &= C(\theta(t))x(t) + D_u(\theta(t))K(\theta(t)) \end{aligned} \tag{19}$$

Before proceeding further, we introduce the following definitions.
Definition 1:[?,?] A unit simplex Θ_r is a polytope of r vertices defined as

$$\Theta_r = \left\{ a = [a_1, a_2, \cdots, a_r] : \quad \sum_{i=1}^{r} a_i = 1, \quad a_i \geq 0, i = 1, 2, ..., r \right\}$$

where variable a_i varies inside a unit simplex Θ_r.
For example, the system matrix $A(\theta)$ can be expressed as

$$A(\theta) = \sum_{i=1}^{r} a_i A_i = A(a), \quad a \in \Theta_r$$

Definition 2:[?] A multi-simplex Θ is the Cartesian product of a finite number of simplexes. For instance, if there are q simplexes, then

$$\Theta = \Theta_{N_1} \times \Theta_{N_2} \times \Theta_{N_3} \times \cdots \Theta_{N_q} = \prod_{i=1}^{q} \Theta_{N_i}\,,$$

where the dimension of multi-simplex Θ is the index $N = (N_1, \ldots, N_q)$, such that a in Θ represents $(a_1, a_2, \ldots, a_q)$ and each a_i in Θ_{Ni} represents $(a_i(1), a_i(2), \ldots, a_i(r))$.

III.A.1. Transferring from affine to multi-simplex

To formulate a convex control design problem, we first need to perform a transformation on the system matrices, from the affine parameter space θ to the multi-simplex convex space Θ. Each affine scheduling parameter θ_i is transferred over a unit simplex a_i as follows,[?]

$$\begin{aligned} a_i(1) &= \frac{\theta_i + \eta_{2,i}}{2\eta_{2,i}} \longrightarrow \theta_i = 2\eta_{2,i}a_i(1) - \eta_{2,i} \\ a_i(2) &= 1 - a_i(1) = 1 - \frac{\theta_i + \eta_{2,i}}{2\eta_{2,i}} = \frac{\eta_{2,i} - \theta_i}{2\eta_{2,i}} \\ a_i &= (a_i(1), a_i(2)) \in \Theta_2, \forall\, i = 1, 2, \cdots, q\,. \end{aligned} \tag{20}$$

With this transformation, the affine scheduling parameters in (12) can be converted into a system with multi-simplex parameters, where the multi-simplex variables are defined as

$$a \in \Theta = \Theta_2 \times \Theta_2 \times \cdots \Theta_2\,.$$

In the case of two scheduling parameters, i.e. $q = 3$, the homogeneous term in the multi-simplex variable can be written as

$$a_1 = (a_1(1), a_1(2)), a_2 = (a_2(1), a_2(2)) \;\text{ and }\; a_3 = (a_3(1), a_3(2))\,.$$

After applying the transformation, Eq.12 and Eq.17 will be in terms of multisimplex variables. Then the closed-loop system can be described by

$$\begin{cases} \dot{x}(t) = A_c(a(t))x(t) + B_w(a(t))w(t) \\ y(t) = C_c(a(t))x(t) + D_w(a(t))w(t) \end{cases} \tag{21}$$

where

$$\begin{aligned} A_c(a(t)) &= A(a(t))x(t) + B_u(a(t))K(a(t)) \\ C_c(a(t)) &= C(a(t))x(t) + D_u(a(t))K(a(t)) \end{aligned} \tag{22}$$

In addition, the time rate change of the scheduling parameters in the unit simplex can also be described by

$$\dot{a}_i(1) + \dot{a}_i(2) = 0, \qquad i = 1, 2, ..., q. \tag{23}$$

From Eqs. (16) and (20) we can derive the rate bounds between affine scheduling parameters and multi-simplex variables, and they are given by

$$\frac{\mu_{1,i}}{2\eta_{2,i}} \leq \dot{a}_i(1) \leq \frac{\mu_{2,i}}{2\eta_{2,i}} \tag{24}$$

where $\mu_{2,i}$ and $\mu_{1,i}$ are rate bounds given in (16), and $\eta_{2,i}$ is the upper bound of θ_i given in (15). Furthermore, from (23), we obtain $\dot{a}_i(2) = -\dot{a}_i(1)$.

III.A.2. $\mathscr{H}_\infty$ control problem

The proposed LPV control problem can be stated as follows:
Design a gain scheduling state-feedback controller of the form $\bar{u}(t) = K(a)x(t)$, such that for a given $\gamma_\infty > 0$ and any given pair $(\alpha, \dot{\alpha})$, the closed-loop system (21) is stabilized and satisfies the following $\mathscr{H}_\infty$ performance constraint,

$$\sup_{(a_i,\dot{a}_i)} \sup_{\substack{w\in l_2 \\ w\neq 0}} \frac{\|z\|_2}{\|w\|_2} < \gamma_\infty \tag{25}$$

To synthesize the $\mathscr{H}_\infty$ control problem, we need the following theorem.
Theorem 1:[?] The gain scheduling controller $K(a) = Z(a)G(a)^{-1}$ stabilizes the closed-loop with guaranteed $\mathscr{H}_\infty$ performance bound γ_∞ for any given pair $(a_i, \dot{a}_i)$, if there exist a scalar $\varepsilon > 0$, a continuously differentiable symmetric and positive-definite matrix $P(a)$, and matrices $G(a)$ and $Z(a)$ satisfying the following parameterized linear matrix inequality (PLMI),

$$\begin{bmatrix} X(a) & * & * & * \\ P(a) - G(a) + \varepsilon(A(a)G(a) + B_u(a)Z(a))' & -\varepsilon(G(a)G(a)') & * & * \\ C(a)G(a) + D_u(a)Z(a) & \varepsilon C(a)G(a) + \varepsilon D_u(a)Z(a) & -I_p & * \\ B_w(a)' & 0_{r\times n} & D_w(a)' & -\gamma_\infty^2 I_r \end{bmatrix} < 0 \tag{26}$$

where $X(a) = A(a)G(a) + B_u(a)Z(a) + G(a)'A(a)' + Z(a)'B_u(a)' + \frac{\partial P(a)}{\partial a}\dot{a}$.

It should be noted that PLMI is an infinite dimensional linear matrix inequality (LMI), which is in general difficult to solve. Many efficient solvers are available in dealing with this problem; for instance, see references.[?,?,?,?] This paper adapts the relaxation method for PLMIs relaxation,[?] where it treats PLMIs with multi-simplex parameters. Numerically, the ROLMIP package[?] along with YALMIP[?] using solver SeDuMi,[?] are used to solve the convex optimization problem.

For three scheduling parameters, the parameters $Z(\theta)$ and $G(\theta)$ in affine θ domain can be described by

$$Z(\theta) = Z_0 + \theta_1 Z_1 + \theta_2 Z_2 + \theta_3 Z_3, \qquad G(\theta) = G_0 + \theta_1 G_1 + \theta_2 G_2 + \theta_3 G_3 \tag{27}$$

where (Z_0, G_0) and (Z_i, G_i), $i = 1, 2, 3$, are constant matrices to be determined in the sequel. Moreover, given $Z(\theta)$ and $G(\theta)$, the affine gain matrix $K(\theta)$ in Eq. (17) will then be given by

$$K(\theta) = Z(\theta)G^{-1}(\theta). \tag{28}$$

Therefore, it is clear that the control gain $K(\theta)$ is not an affine function of θ. For three scheduling parameters, there are 8 polytopic solutions for $Z(a)$ and $G(a)$ in Eq. (26). Let $\mathscr{Z}_{ijk}$ and $\mathscr{G}_{ijk}$, $i,j,k=1,2$, to denote these solutions, then $Z(a)$ and $G(a)$ can be represented as

$$\begin{aligned} X(a) = {} & a_1(1)a_2(1)a_3(1)\mathscr{X}_{111} + a_1(1)a_2(1)a_3(2)\mathscr{X}_{112} \\ & + a_1(1)a_2(2)a_3(1)\mathscr{X}_{121} + a_1(1)a_2(2)a_3(2)\mathscr{X}_{122} \\ & + a_1(2)a_2(1)a_3(1)\mathscr{X}_{211} + a_1(2)a_2(1)a_3(2)\mathscr{X}_{212} \\ & + a_1(2)a_2(2)a_3(1)\mathscr{X}_{221} + a_1(2)a_2(2)a_3(2)\mathscr{X}_{222} \\ = {} & X(\theta) \end{aligned} \tag{29}$$

where $(X,\ \mathscr{X})$ represents $(Z,\ \mathscr{Z})$ or $(G,\mathscr{G})$. Hence, it follows from the inverse transformation process given in[?] that

$$X_0 = \frac{1}{2^{2q}} \sum_{j_1=1}^{2} \cdots \sum_{j_q=1}^{2} \sum_{k_i=1}^{2} \cdots \sum_{k_q=1}^{2} \mathscr{X}_{j_1,\ldots,j_q,k_1,\ldots,k_q}\,, \tag{30}$$

$$X_i = \frac{1}{2^{2q}\bar{\theta}_i} \sum_{j_1=1}^{2} \cdots \sum_{j_q=1}^{2} \sum_{k_i=1}^{2} \cdots \sum_{k_q=1}^{2} (-1)^{j_i+i} \mathscr{X}_{j_1,\ldots,j_q,k_1,\ldots,k_q}\,. \tag{31}$$

where the matrices (X_0, X_i) represents (Z_0, Z_i) or (G_0, G_i), and $\mathscr{X}_{j_1j_2j_3}$ denotes the polytopic solutions $\mathscr{Z}_{j_1j_2j_3}$ or $\mathscr{G}_{j_1j_2j_3}$ from Theorem 1. Now, substituting (Z_0, Z_i) and (G_0, G_i) into Eq. (27) yields $Z(\theta)$ and $G(\theta)$, hence the feedback gain matrix $K(\theta)$ can be obtained from Eq. (28)

IV. Simulation Investigation

The baseline LPV-0 controller and the proposed LPV-1 controller are designed based upon their corresponding models, with γ_∞ chosen to be 0.0055 in Theorem 1. In this simulation analysis, the airspeed is varying from 4m/s to 23.8m/s. The gain matrices of the resulting LPV-0 controller (Z_{00}, G_{00}) and (Z_{i0}, G_{i0}) are:

$$\begin{aligned} Z_{00} &= [-0.051788000,\ \ 0.2853700, -0.261390,\ \ 0.476160,\ \ 0.045888, -8.81260], \\ Z_{20} &= [-0.000028579,\ \ 0.0095015, -0.036397,\ \ 0.083472, -0.018931, -0.63590], \\ Z_{30} &= [\ \ 0.008960500, -0.1393600,\ \ 0.006209, -0.042522, -0.117880,\ \ 0.31722]. \end{aligned} \tag{32}$$

$$G_{00} = \begin{bmatrix} 1.0292e-05 & -7.0926e-06 & -2.0329e-07 & 3.6702e-06 & 7.1505e-09 & -9.4204e-05 \\ -7.032e-06 & 3.6004e-05 & -2.4069e-06 & -2.6686e-06 & -4.575e-06 & 3.9664e-04 \\ -4.1334e-07 & -2.1419e-06 & 1.0487e-05 & -1.3243e-05 & 9.1849e-05 & 4.0045e-05 \\ 3.9355e-06 & -3.5161e-06 & -1.3181e-05 & 4.2533e-05 & -3.7746e-04 & -1.4701e-04 \\ -1.6558e-06 & 2.3264e-06 & 9.6502e-05 & -3.961e-04 & 4.9923e-02 & -3.2631e-01 \\ -9.4264e-05 & 3.9815e-04 & 1.1691e-05 & -3.0011e-05 & -3.288e-01 & 104.92e-01 \end{bmatrix} \tag{33}$$

$$G_{20} = \begin{bmatrix} 1.0241e-05 & -6.8766e-06 & -1.9139e-07 & 3.642e-06 & -7.7403e-08 & -9.4036e-05 \\ -6.8168e-06 & 3.54e-05 & -2.4457e-06 & -2.648e-06 & -3.9416e-07 & 3.8971e-04 \\ -4.0415e-07 & -2.17e-06 & 1.063e-05 & -1.3519e-05 & 9.2068e-05 & 2.5043e-05 \\ 3.9103e-06 & -3.5054e-06 & -1.3456e-05 & 4.2983e-05 & -3.792e-04 & -9.1409e-05 \\ -2.0406e-06 & 7.7154e-06 & 9.6801e-05 & -3.982e-04 & 5.1528e-02 & -2.3771e-01 \\ -9.4179e-05 & 3.9065e-04 & 4.2126e-06 & -5.6076e-06 & -2.52e-01 & 29.561e-01 \end{bmatrix} \tag{34}$$

$$G_{30} = \begin{bmatrix} 1.0241e-05 & -6.8766e-06 & -1.9139e-07 & 3.6419e-06 & 3.0065e-08 & -9.4368e-05 \\ -6.8168e-06 & 3.54e-05 & -2.4457e-06 & -2.648e-06 & -8.4001e-07 & 3.9108e-04 \\ -4.0415e-07 & -2.17e-06 & 1.063e-05 & -1.3519e-05 & 9.2005e-05 & 2.5621e-05 \\ 3.9103e-06 & -3.5054e-06 & -1.3456e-05 & 4.2983e-05 & -3.7894e-04 & -9.4228e-05 \\ -2.0393e-06 & 7.7183e-06 & 9.681e-05 & -3.9823e-04 & 5.2281e-02 & -2.4613e-01 \\ -9.4195e-05 & 3.9049e-04 & 3.9802e-06 & -4.9266e-06 & -2.6559e-01 & 30.102e-01 \end{bmatrix} \tag{35}$$

and the gain matrices of the resulting LPV-1 controller (Z_{01}, G_{01}) and (Z_{i1}, G_{i1}) are:

$$\begin{aligned}
Z_{01} &= [\ \ 0.548420, -0.00019372, -0.15522000, \ \ 0.71419000, \ \ 1.08060000, -109.9000], \\
Z_{11} &= [\ \ 0.553410, -0.00019562, -0.13229000, \ \ 0.70671000, \ \ 1.08980000, -110.8800], \\
Z_{21} &= [-0.014035, -0.03191200, \ \ 0.08397600, -0.05061400, -0.00059914, -0.048978], \\
Z_{31} &= [-0.287940, -0.00022911, \ \ 0.00022877, -0.00082886, \ \ 0.02613200, -0.121390].
\end{aligned} \tag{36}$$

$$G_{01} = \begin{bmatrix}
7.8896e-06 & -4.88e-06 & -2.1003e-07 & 3.0824e-06 & -4.144e-05 & -3.9649e-05 \\
-4.8329e-06 & 2.7367e-05 & -1.6313e-06 & -3.1912e-06 & 1.3371e-04 & 2.3919e-04 \\
-3.6471e-07 & -1.4518e-06 & 7.9214e-06 & -9.6416e-06 & 8.1299e-05 & -5.8287e-05 \\
3.2593e-06 & -3.784e-06 & -9.5948e-06 & 3.2516e-05 & -3.6529e-04 & 7.8805e-05 \\
-4.2384e-05 & 1.3887e-04 & 8.1301e-05 & -3.6761e-04 & 1.8855e-02 & -5.0645e-01 \\
-2.8195e-05 & 1.7853e-04 & -5.6427e-05 & 1.6936e-04 & -5.1254e-01 & 507.95e-01
\end{bmatrix} \tag{37}$$

$$G_{11} = \begin{bmatrix}
7.8884e-06 & -4.8753e-06 & -2.0747e-07 & 3.0788e-06 & -4.1397e-05 & -3.9695e-05 \\
-4.8288e-06 & 2.7344e-05 & -1.6295e-06 & -3.1935e-06 & 1.3359e-04 & 2.3879e-04 \\
-3.6188e-07 & -1.4515e-06 & 7.9138e-06 & -9.6322e-06 & 8.1284e-05 & -5.8183e-05 \\
3.2555e-06 & -3.7846e-06 & -9.5862e-06 & 3.2506e-05 & -3.6529e-04 & 7.8771e-05 \\
-4.2359e-05 & 1.388e-04 & 8.1281e-05 & -3.6761e-04 & 1.8855e-02 & -5.0643e-01 \\
-2.8291e-05 & 1.7829e-04 & -5.63e-05 & 1.6924e-04 & -5.1253e-01 & 507.95e-01
\end{bmatrix} \tag{38}$$

$$G_{21} = \begin{bmatrix}
7.8555e-06 & -4.7094e-06 & -2.0663e-07 & 3.0568e-06 & -4.0963e-05 & -2.6925e-06 \\
-4.6633e-06 & 2.6788e-05 & -1.6547e-06 & -3.1241e-06 & 1.3399e-04 & 8.7094e-05 \\
-3.6405e-07 & -1.4649e-06 & 8.0632e-06 & -9.8762e-06 & 8.1091e-05 & -6.0543e-05 \\
3.2368e-06 & -3.726e-06 & -9.8281e-06 & 3.2861e-05 & -3.6601e-04 & 1.9392e-04 \\
-4.1803e-05 & 1.3851e-04 & 8.111e-05 & -3.6749e-04 & 1.398e-02 & -1.305e-02 \\
-2.1645e-06 & 8.5489e-05 & -6.2007e-05 & 1.9973e-04 & -1.3281e-02 & 2.3088e-02
\end{bmatrix} \tag{39}$$

$$G_{31} = \begin{bmatrix}
7.8543e-06 & -4.7047e-06 & -2.0406e-07 & 3.0532e-06 & -4.092e-05 & -2.7393e-06 \\
-4.6591e-06 & 2.6765e-05 & -1.6529e-06 & -3.1264e-06 & 1.3387e-04 & 8.6695e-05 \\
-3.6122e-07 & -1.4646e-06 & 8.0557e-06 & -9.8668e-06 & 8.1075e-05 & -6.0439e-05 \\
3.2329e-06 & -3.7267e-06 & -9.8195e-06 & 3.2851e-05 & -3.66e-04 & 1.9388e-04 \\
-4.1778e-05 & 1.3845e-04 & 8.109e-05 & -3.6748e-04 & 1.398e-02 & -1.3033e-02 \\
-2.2601e-06 & 8.525e-05 & -6.188e-05 & 1.9961e-04 & -1.3264e-02 & 2.305e-02
\end{bmatrix} \tag{40}$$

Simulation results are compared with those obtained from the nonlinear controller presented in Ref.[?] Figure 4 shows a comparison between the proposed LPV-1 controller and the nonlinear controller,[?] with small initial pitch angle, i.e. $\alpha_S = 0.01$rad. It can be clearly observed that the proposed LPV-1 control can significantly improve the overall closed-loop performance over the nonlinear control strategy proposed in Ref.[?]

As mentioned, the control mass m is confined to move within the groove between -0.5 and 0.5. In the proposed LPV-1 control design technique, the scheduling parameter θ_1 is used to constrain the mass movement. Figure 5 shows the same comparisons but with larger initial pitch angle at $\alpha_L = 0.6$rad. It is apparent that the nonlinear controller from Ref.[?] cannot handle the large angle of attack, while the proposed LPV-1 control design handles this condition very effectively, with fast convergence and small control effort.

Figure 6 shows a comparison between the LPV-1 controller and the baseline LPV-0 controller. Recall that in LPV-0 control design, no position limitation is imposed on the moving mass m. Therefore, as can be seen in Fig. 6, for LPV-0 controller to be effective in suppressing airfoil vibration, the control mass needs a very large displacement.

A quantitative study of the results, by considering the $\|.\|_\infty$ and $\|.\|_2$ norms of the signals, are presented in Tables 2, 3, and 4. Table 2 shows the comparison between the $\|.\|_\infty$ norms of the proposed design technique and Ref.[?] with small

and large initial conditions. It is clear that the improvement is more than 50% for most of the system performance related norms, with nearly 50 time less control effort. A comparison between $\|.\|_\infty$ norms of the proposed design technique LPV-1 and baseline LPV-0 is presented in Table 3.

Table 4 shows a comparison between $\|.\|_2$ of the proposed design technique and that of Ref.[?] with small and large initial conditions. It is clear that the proposed design technique provides much faster convergent rate; see the percentage of improvement in the last column.

Table 2: Comparison of the proposed controller (LPV-1) with one from Ref.[?]

Case	$\|.\|_\infty$	Ref.[?]	Proposed LPV-1
Small Initial Conditions	$\bar{h}$	0.0040099	0.0029746
	α	0.01	0.01
	$\bar{y}$	0.24058	0.083381
	$\bar{u}$	0.23176	0.18602
Large Initial Conditions	$\bar{h}$	0.24444	0.29736
	α	0.6	0.6
	$\bar{y}$	0.86839	0.4705
	$\bar{u}$	619.82	11.347

Table 3: Comparison of the proposed controller (LPV-1) with LPV-0.

Case	$\|.\|_\infty$	LPV-0	LPV-1
Large initial conditions	$\bar{h}$	0.14294	0.29736
	α	0.6	0.6
	$\bar{y}$	7.8091	0.4705
	$\bar{u}$	47.979	11.347

Table 4: Comparison of the proposed controller (LPV-1) with one from Ref.[?]

Case	$\|.\|_2$	Ref.[?]	Proposed LPV	Convergent rate%
Small initial conditions	$\bar{h}$	0.4946	0.20804	57
	α	0.98788	0.38593	60
	$\bar{y}$	28.36	4.0848	85
	$\bar{u}$	26.744	11.359	57
Large initial conditions	$\bar{h}$	30.216	27.771	8
	α	60.868	45.592	25
	$\bar{y}$	254.07	115.57	54
	$\bar{u}$	6802.3	519.59	92

V. Conclusions

This paper proposes a novel LPV modeling and control design technique for a smart airfoil model that utilizes a moving mass for flutter suppression. The LPV gain-scheduling state-feedback controllers based on the corresponding models are proposed, in which the moving mass position is used as the scheduling parameter. The performance of the proposed LPV controllers is compared with an earlier nonlinear controller from the literature, and the results clearly demonstrate the advantages and the effectiveness of the proposed LPV modeling and control design techniques in active flutter suppression. Future research includes experimental testing of the proposed concept and utilization of switched LPV control techniques.

Acknowledgement

The authors would like to thank the funding support of NASA ARMD Convergent Aeronautics Solutions (CAS) project. Ali M. H. Al-Hajjar also would like to thank the Higher Committee For Education Development (HCED) and University of kufa for his Ph.D. support.

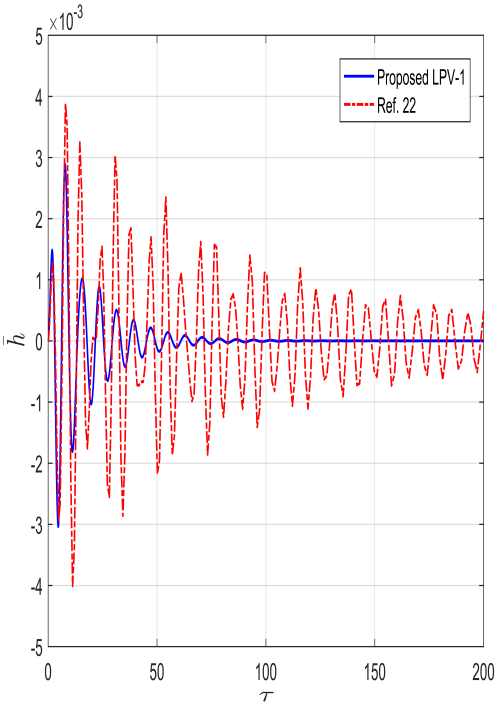

(4:a)

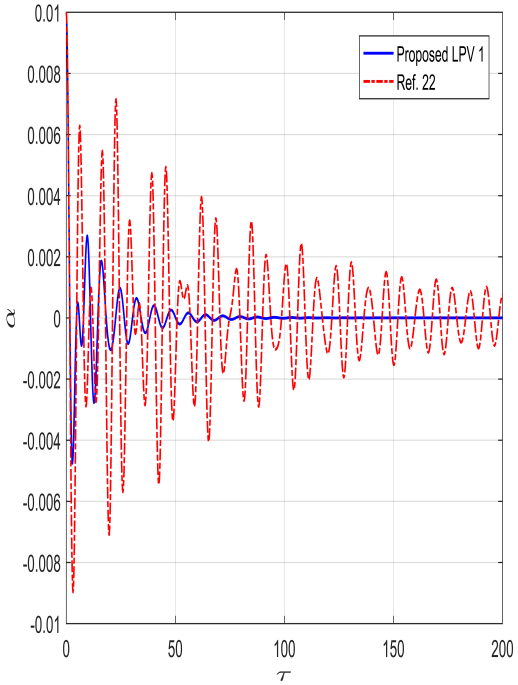

(4:b)

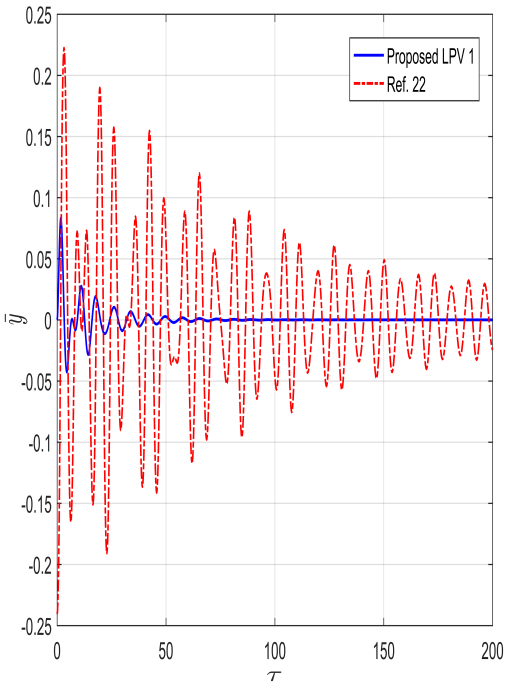

(4:c)

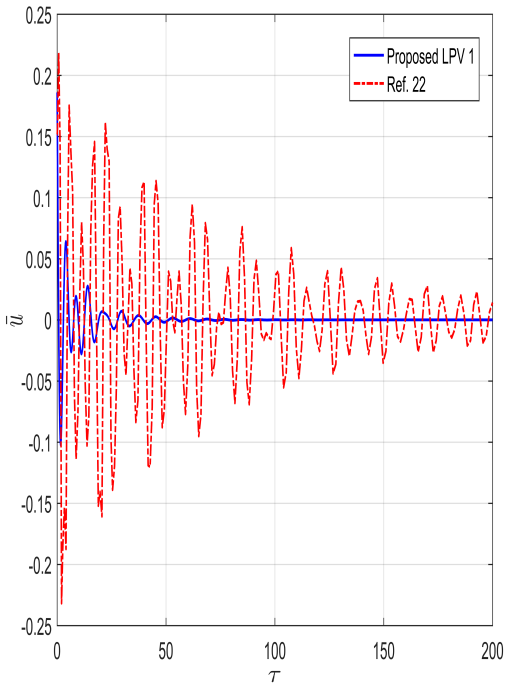

(4:d)

Figure 4: Comparison between proposed LPV-1 control and Ref.,? Small initial condition.

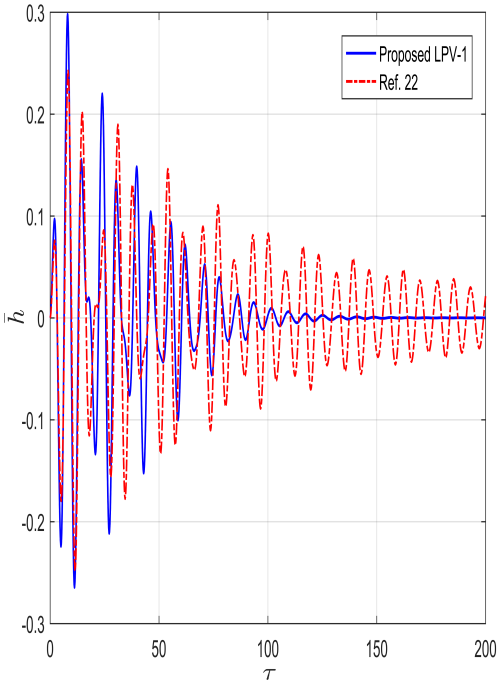

(5:a)

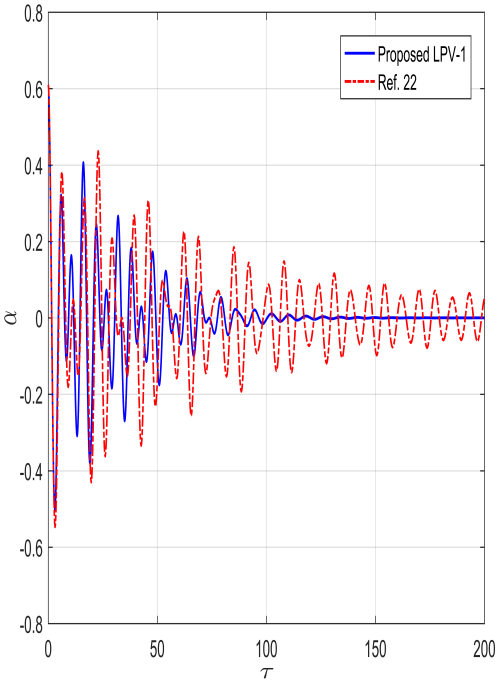

(5:b)

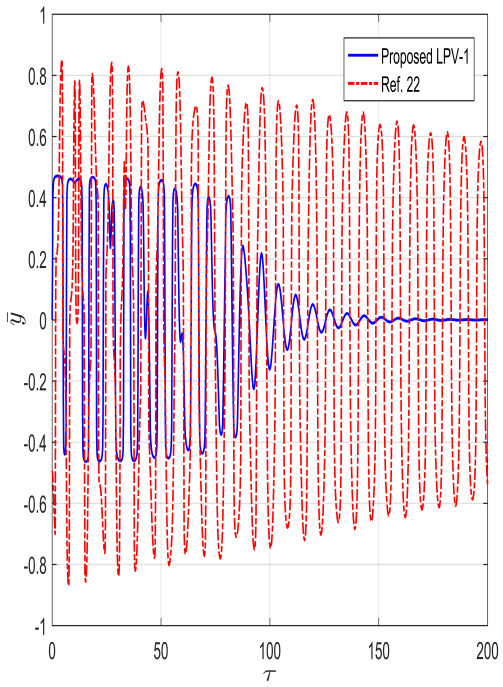

(5:c)

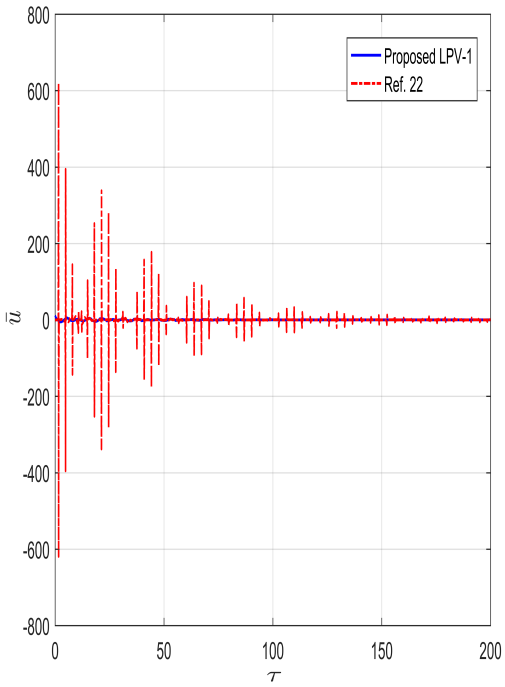

(5:d)

Figure 5: Comparison between proposed LPV-1 control and Ref.,? Large initial condition.

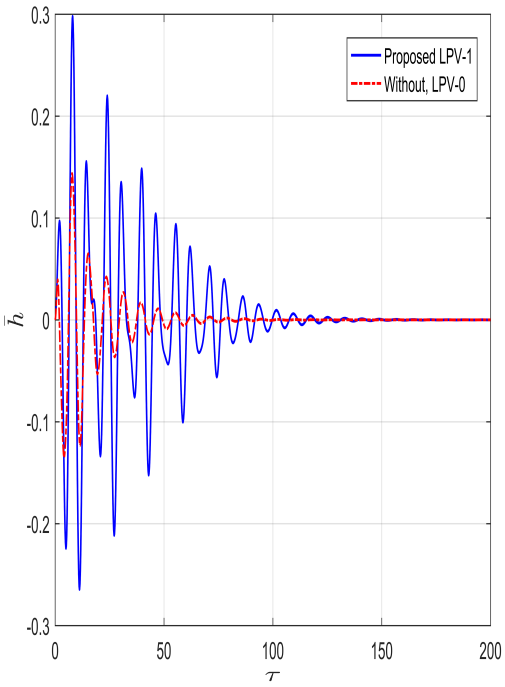

(6:a)

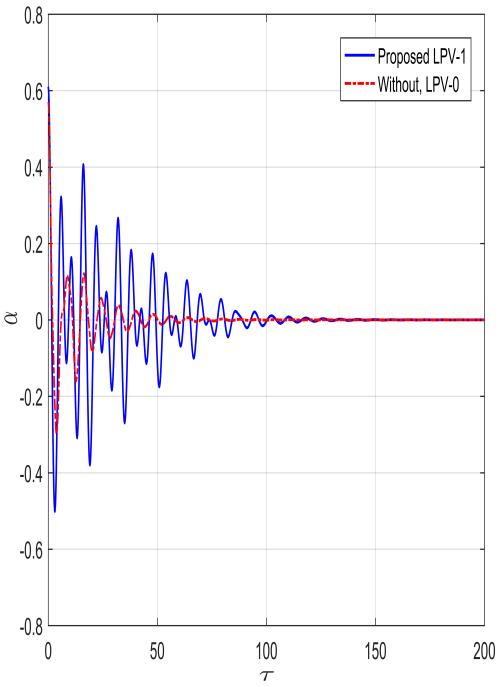

(6:b)

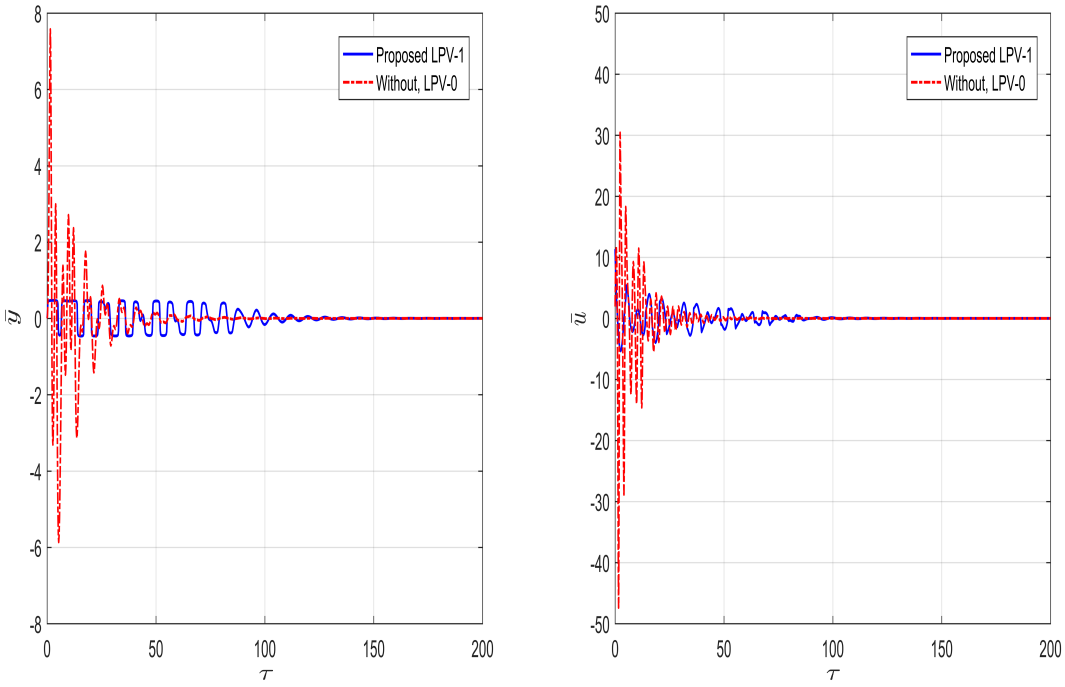

(6:c) (6:d)

Figure 6: Comparison between LPV-1 control and LPV-0 control, Large initial condition.